

Preparation of Stearic Acid/Graphene Oxide Based Form-Stable Composite Phase Change Materials

Stearik Asit/Grafen oksit Esaslı Form-Kararlı Kompozit Faz Değişim Malzemelerinin Hazırlanması

Burcu OKTAY^{ID}

Marmara Üniversitesi, Kimya Bölümü, 34722, İstanbul, Türkiye

Abstract

Composite phase change materials (PCM) of stearic acid/graphene oxide were prepared by thiol-alkyne click coupling reaction. Stearic acid was firstly modified with propargyl to introduce thiol-yne clickable sites. Different amounts of graphene oxide were added to thiol-alkyne clickable formulation. To evaluate phase change properties of PCMs differential scanning calorimeter (DSC) was used. Thermal stability and degradation profiles of PCMs were investigated. The structural characterization of stearic propargyl ester and PCMs was performed by ATR-FTIR spectroscopy. The addition of graphene oxide increased the maximum weight loss temperature from 328 to 351 °C with respect to the base formulation. Moreover, the crosslinking of stearic acid prevented the leakage of PCMs.

Keywords: Phase change materials, thiol-yne click, graphene oxide

Öz

Stearik asit-grafen oksit kompozit faz değişim malzemeleri (PCM) tiyol-alkin klik kapanma reaksiyonu ile hazırlandı. Öncelikle stearik asit tiyol-yne klik gruplarının bağlanması amacıyla modifiye edildi. Farklı miktarlarda grafen oksit tiyol-klik formülasyonuna eklendi. PCM'lerin faz değişim özelliklerini incelemek için diferansiyel taramalı kalorimetre (DSC) kullanıldı. PCM'lerin termal kararlılık ve bozunma profili incelendi. Stearik propargyl esteri ve PCM'lerin yapısal karakterizasyonu ATR-FTIR spektroskopisi ile gerçekleştirildi. Grafen oksit eklenmesiyle baz formülasyona göre maksimum kütle kaybı sıcaklığı 328 dan 351 °C ye yükseldi. Aynı zamanda stearik propargyl çapraz bağlanmasıyla PCM'lerin akma problemi engellendi.

Anahtar Kelimeler: Faz değişim malzemeleri, tiyol-yne klik, grafen oksit

I. INTRODUCTION

Rapid development and growth of population reveal the need for energy. Hence, the storage of thermal energy has become an important area in modern technology. Phase change materials (PCMs) are a kind of thermal energy storage materials. PCMs have high energy storage density and can store energy in isothermal process. In addition, PCMs show extremely small temperature variation during charging and discharging processes [1]. PCM technology has been used for many fields such as solar energy storage and transfer systems, heat storage cloths and industrial waste heat recovery [2]. PCMs can be divided in three categories; inorganic compounds, organic compounds and eutectic mixtures [3]. Inorganic PCMs contain hydrate salts, metals and alloy, which have high volumetric heat storage capacity and good thermal conductivity. However, their applications are restricted because of their super cooling and phase decomposition [4].

Organic PCMs can be categorized into two major categories: paraffin (hydrocarbons) and non-paraffinic (fatty acids and their derivatives) based materials. Fatty acids have superior properties such as chemical stability, melting congruency,

non-toxicity and high latent heat compared to other available PCMs. Furthermore, another advantage of fatty acids there are abundantly available due to derive from common vegetable and animal oils. The Capric acid, Lauric acid, Palmitic acid and Stearic acid are majorly studied fatty acids [5].

There are some works, which consider the use of fatty acids in PCMs. For instance, Alva et al. prepared myristic acid–palmitic acid (MA–PA) eutectic mixture with silica shell and characterized by differential scanning calorimeter (DSC) [6]. Zhang et al. prepared stearic acid/polymethylmethacrylate (PMMA) PCMs. The latent heats of PCMs with stearic acid percentage of 52.20 wt% are 102.1 and 102.8 J/g at 55.3 and 48.8 °C, respectively [7]. Doğüşcü et al. investigated palmitic acid (PA) and capric acid (CA) eutectic composition ratio of the mixture. The phase change temperatures and latent enthalpies of PCMs were determined using DSC found between 13.5–17.9 °C and 45.0–77.3 J/g, respectively [8].

Among fatty acids, stearic acid has a suitable phase change materials. Literature survey shows that the thermal characteristics of stearic acid and its esters indicated available for heat storage in buildings [9]. However, stearic acid tends to leakage when melting. Leakage is an important problem for PCMs, which limits their usage area [10]. Several preparation techniques have been used to overcome this problem such as encapsulation, photopolymerization [11], embedding like metal particles and fatty alcohol into PCMs [12].

Carbon nanomaterials such as carbon nanotube, graphene, graphene oxide exhibit high stability and thermal conductivity as well as low density. The excellent properties of carbon nanomaterials make them suitable additives for PCMs. Graphene oxide is an oxygen-rich carbonaceous layered material, which is composed by sp³-hybridized carbons and sp²-hybridized carbons. Graphene oxide can interact with hydrophilic groups of polymers through hydrogen bonding. Also, graphene oxide has a physical crosslinking agent to obtain interacting polymer [13].

Zhong et al. prepared composite PCMs consisting graphene oxide and octadecanoic acid. The thermal conductivity of the composite PCM was about 14 times than that of pure octadecanoic acid [14]. Cui et al. obtained carbon nanotube and carbon nanofiber containing soy wax and paraffin wax PCMs. The thermal conductivity of composite PCMs increases with addition of carbon nanotube and carbon nanofiber [15]. Li et al. expanded graphite and carbon nanotube added into stearic acid. The composite PCMs were prepared via melt blending. The increasing of carbon nanomaterials content from 1 to 9% thermal conductivity increased [10]. Based on the literature described above, thermal conductivity and thermal stability of the composite PCMs considerably enhance

with addition carbon nanomaterial. The phase change temperature of composite PCMs stays almost the same. The latent heat of composite PCMs very little decreases but is still preserve its high latent heat storage ability. In addition, leakage of composite PCMs is greatly prevented with the addition of carbon nanomaterials.

The objective of our study is to prepare crosslinked stearic acid network via thiol-alkyne photopolymerization and investigate the effect of different amount of graphene oxide on the latent heat of composite PCMs. Propargyl groups bearing stearic acid was firstly synthesized to obtain thiol-alkyne clickable network. Photo-curable PCMs were prepared by mixing propargyl stearic acid, 3SH, different amount of graphene oxide and photoinitiator (DMPA). The chemical structures of PCMs were investigated by means of ATR–FTIR technique. Thermal properties and phase transition behaviors of the nanofiber based PCMs were determined by TGA and DSC.

II. MATERIALS AND METHODS

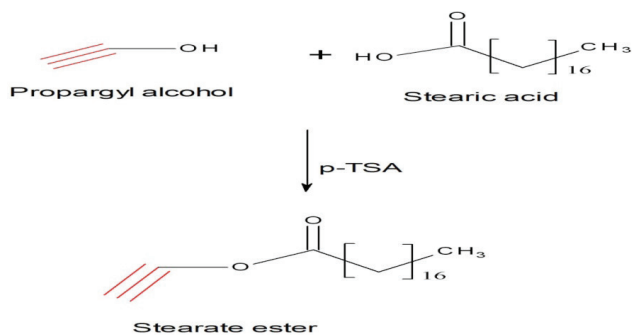
2.1. Reagents and Apparatus

Propargyl alcohol (99%), stearic acid, trimethylpropanetrakis(3-mercaptopropionate) ($\geq 95.0\%$) (3SH), 2,2-dimethoxy-2-phenylacetophenone (99%) (DMPA), graphene oxide (4 mg/mL, dispersion in H₂O), p-toluensulfonic acid (98%) (p-TSA) were purchased from Aldrich.

The structure of ester of stearic acid was identified by Attenuated Total Reflection Fourier Transform Infrared spectroscopy (ATR-FTIR). The spectra were collected using a Perkin Elmer Spectrum 100 ATR-FTIR spectrophotometer. The spectrums were recorded over a scanning range of 4000 and 400 cm⁻¹. Thermal properties of PCMs were examined by Thermal Gravimetric Analysis (TGA) using a Perkin-Elmer Thermogravimetric analyzer STA6000 model. TGA curves of the nanofibers were obtained in the 30 - 750 °C temperature range with heating rate of 10 °C/min under air and nitrogen atmospheres. Phase change properties and phase transitions of PCMs were examined by Pyris Diamond differential scanning calorimeter (DSC). DSC analysis was run from 0 °C to 80 with 5 °C/min heating and cooling rates under nitrogen at 25 ml/min.

2.2. Synthesis of stearate ester

Stearic acid (0.035 mol) and propargyl alcohol (0.17 mol) were stirred at 80 °C in the presence of toluene-4-sulfonic acid (0.052 mmol) in 25 mL THF for 24 h. After 24 h, the mixture was washed with water to remove un-reacted propargyl alcohol and toluene-4-sulfonic acid. Then THF was removed by evaporation and the product was dried in vacuum. The synthesis pathway of stearic propargyl ester shows in Scheme 1.

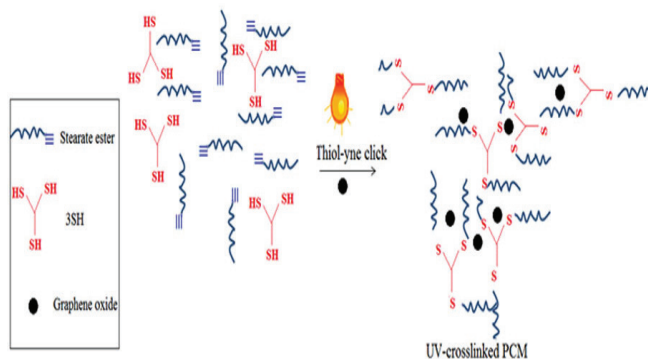


2.3. Preparation of PCMs

All thiol-yne reaction was carried out in Argon filled glove box. Thiol-yne clickable base formulation (P-0) was prepared by mixing stearate ester, 3SH monomer with DMAP as a photoinitiator in a beaker. The mixture was irradiated with 365 nm light (120 W/cm², distance between lamp and surface was 15 cm, OSRAM, Turkey) for 1 h to promote the thiol-yne click reaction. P-5 formulation was prepared by adding %5 wt. graphene oxide to the base formulation (P-0). The mixture was sonicated by ultrasonicator (Baneline HD3110) for 15 minutes and then irradiated as described above. P-10 and P-15 formulations were prepared by adding of 10 and 15wt.% graphene oxide, respectively. An illustration of the thiol-yne click reaction can be seen in Scheme 2. The composition of all formulations is given in Table 1.

Table 1. Formulation of thiol-yne samples

Samples	Stearate ester (g)	3SH (g)	Graphene oxide (%)	Graphene oxide (g)
P-0	0.25	0.2	0	-
P-5	0.25	0.2	5	0.60
P-10	0.25	0.2	10	0.13
P-15	0.25	0.2	15	0.25



III. RESULTS

3.1. Structural characterizations

Stearate ester was synthesized by reacting propargyl alcohol and stearic acid in the presence of p-TSA. The structure was characterized via FTIR spectroscopy. Figure 1 shows the FTIR spectrum of the stearic acid, propargyl alcohol and synthesized fatty acid propargyl ester, respectively.

In FTIR spectrum of stearic acid (in black), the bands at 2954, 2914 and 2847 cm⁻¹ correspond to the asymmetric and symmetric stretching vibration of CH. The carbonyl groups of stearic acid observed was observed at 1700 cm⁻¹. The characteristic the alkyne peaks of propargyl alcohol (≡C-H and C≡C) observe about 3290 and 2122 cm⁻¹, respectively [16]. These peaks of the characteristic propargylalcohol are also present in the spectrum of fatty acid propargyl ester (in blue). The peaks at 3290 and 2120 cm⁻¹ correspond to the alkyne peaks of propargyl. The asymmetric stretching of -CH₃, as well as symmetric and asymmetric -CH₂ stretching vibrations of stearic acid were observed at 2951, 2910 and 2848 cm⁻¹. The peaks at 1742 and 1702 cm⁻¹ are attributed to -carbonyl band because of the formation of fatty acid ester [17].

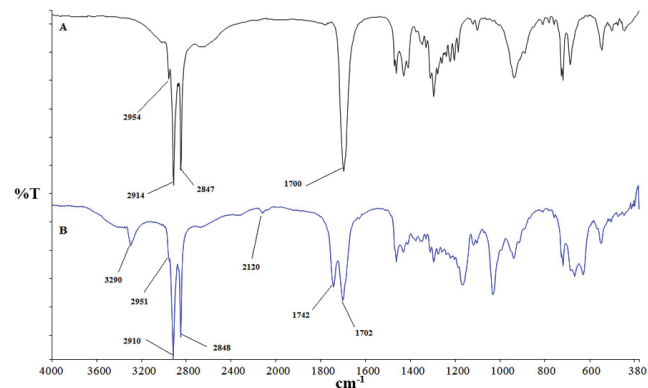


Figure 1. FTIR spectra of (A) stearic acid and (B) stearate ester

3.2. Thiol-yne click reaction

Thiol-yne click reaction occurs between propargyl groups of fatty acid ester and thiol group of 3SH in the presence of DMPA. The overlapped FTIR spectra of P-0, P-5, P-10 and P-15 as well as P-0 of before UV-treatment are shown in Figure 2. In the spectrum A, the peaks at 3286 and 2120 cm⁻¹ correspond to the stretching vibration of H-C and C≡C, respectively [18]. The thiol groups observed at 2550-2600 cm⁻¹.

In the spectrum of P-0 (spectrum B), the bands at 2954, 2914 and 2847 cm⁻¹ correspond to the asymmetric stretching of -CH₃ and symmetric and asymmetric -CH₂ stretching

vibrations, respectively. Ester carbonyl band was observed at 1700 cm^{-1} [17]. In the spectrum C, the peak 1604 cm^{-1} belonging to in-plane vibrations of the skeletal C=C band of hexagonal aromatic ring on the graphene oxide. The peaks at 3026 cm^{-1} corresponding to aromatic =C-H stretching [19]. The characteristic peaks of stearic acid were also observed at about 3026 , 2922 , 2852 and 1738 cm^{-1} the all spectrum.

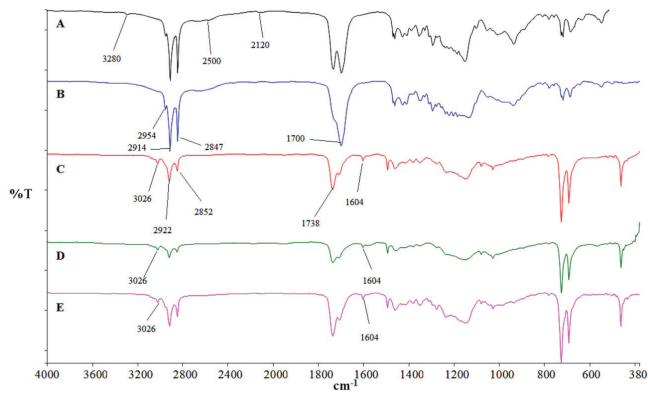


Figure 2. FTIR spectra of (A) P-0, (B) P-5, (C) P-10, (D) P-15 and (E) P-0 of before UV-treatment

3.3. Thermal Properties of PCMs

Figure 3, Figure 4 and Table 2 show thermal degradation profiles of composite PCMs (P-0, P-5, P-10 and P-15) under inert and oxidative atmospheres, respectively. Corresponding derivative curves are also presented in these figures. It can be seen from figure that the 50% weight loss temperature was 332, 335, 345 and 352 °C, respectively under nitrogen atmosphere. 50% weight loss increase slightly with increasing of graphene oxide. Moreover, the char yields increased gradually as the graphene oxide content was increased. In oxidative conditions, graphene oxide was improved 50% weight loss temperature of P-0, P-5, P-10 and P-15. It is clearly that the addition of graphene oxide has a significant contribution to the thermal stability of the PCMs as 20 and 23 degrees of increase was observed in the 50% weight loss temperature of P-15 compared to P-0.

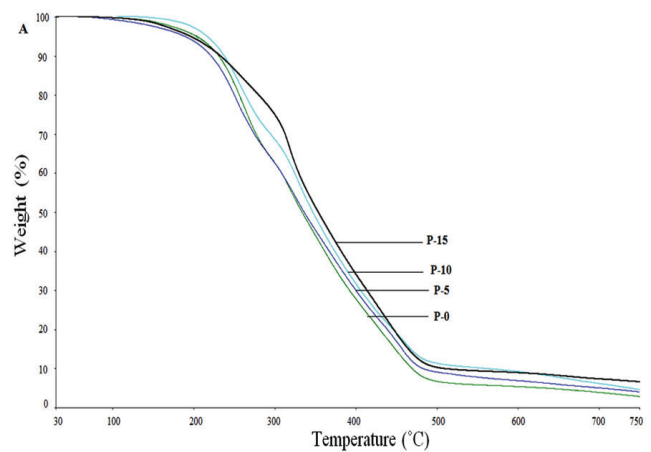


Figure 3A. TGA curves of the composite PCMs, in nitrogen atmosphere

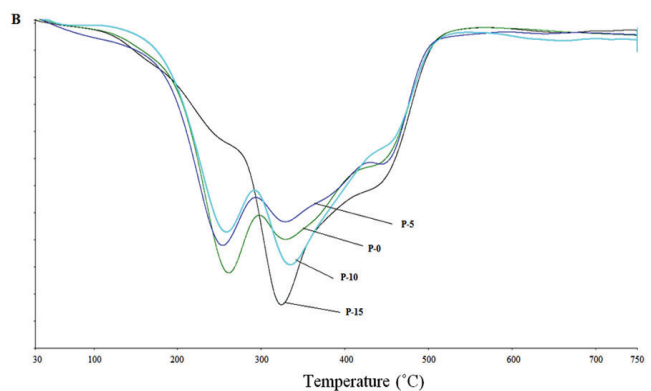


Figure 3B. DTG curves of the composite PCMs, in nitrogen atmosphere

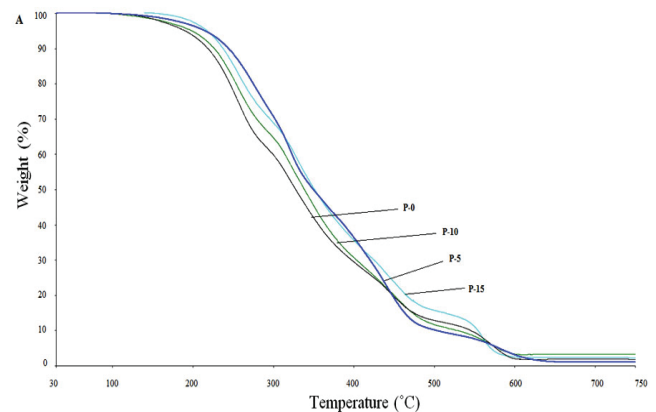


Figure 4A. TGA curves of the composite PCMs, in air atmosphere

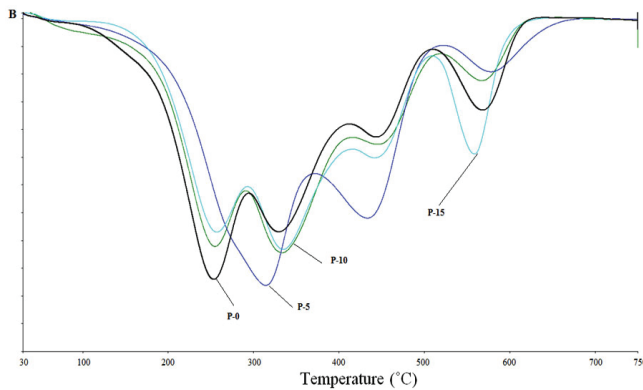


Figure 4B. DTG curves of the composite PCMs, in air atmosphere

Table 2. Thermal properties of composite PCMs

Samples	INERT			AIR		
	T5% (°C)	T50% (°C)	Char (%)	T5% (°C)	T50% (°C)	Char (%)
P-0	203	332	2.96	188	328	1.88
P-5	190	335	4.66	217	346	2.32
P-10	218	345	4.15	198	338	3.00
P-15	194	352	6.62	216	351	3.24

3.4. Phase Transition Properties of PCMs

Figure 5 shows DSC curves of pure stearic acid and propargyl ester of stearic acid. The corresponding data of melting peak temperature (T_m), enthalpy of melting (ΔH_m), crystallization peak temperature (T_c), and enthalpy of crystallization (ΔH_c) are shown in Table 3. Pure stearic acid exhibits single phase change at 61°C. The latent heats of melting is 178 J/g. However, propargyl ester of stearic acid showed two melting peaks at 21 and 58 °C. Moreover the fattyacidester has considerably high latent heat of melting as a 65 and 203 J/g compare to pure stearic acid. The total amount of two latent heats is 268 J/g during melting. As can be seen from DSC results the melting points between stearic acid and its ester changed. The physical properties of a chemical compound affected to the melting point. Knothe et al. investigated and reported for melting points of some compounds. For example, the melting point difference between pure stearic acid and methyl-branched stearic acid ester is about 31.7 °C [20].

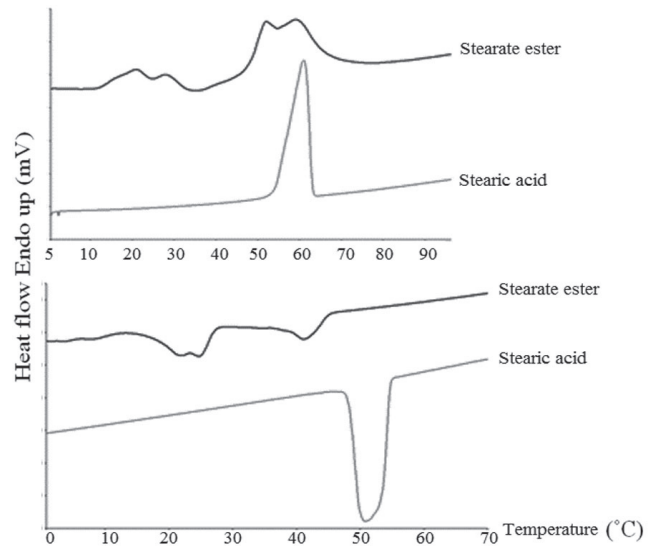


Figure 5: DSC curves of pure stearic acid and ester of stearic acid

Table 3. Latent heat storage properties of stearic acid, stearic ester and the composite PCMs

Samples	T_{m1}	T_{m2}	ΔH_{m1}	ΔH_{m2}	T_{c1}	T_{c2}	ΔH_{c1}	ΔH_{c2}
Stearic acid	-	61	-	178	-	51	-174	-
Stearate ester	21	58	65	203	25	41	-50	-22
P-0	14	61	11	39	7	43	-6	-40
P-5	20	54	14	30	10	42	-11	-28
P-10	22	56	11	23	14	46	-12	-21
P-15	22	52	13	18	7	43	-6	-26

The heating and freezing phase change enthalpy of thiol-yne clicked PCMs were investigated via differential scanning calorimeter and the results are listed in Table 2. As can be seen Figure 6, the melting temperature peaks (T_m) of P-0 were 14 and 61 °C. The latent heat of melting was 50 J/g. For freezing process, the latent heat of P-0 was 46 J/g. While 5 percent adding grapheneoxide, the melting peaks of P-5 were found 20 and 54 °C. The peaks shift to 20 and 54 °C because of the influence of the graphene oxide framework [21]. The latent heat of P-10 was 44 J/g, which decreases a little after adding graphene oxide. For freezing process, the latent heat of SAT-5 was 39 J/g. The latent heat of P-15 in melting and freezing process was 34 and 33 J/g, respectively. The melting temperatures of P-15 were 22 and 56 °C and the freezing temperatures of P-15 were 14 and 46 °C. The melting and freezing temperatures of composite PCMs are suitable for low temperature energy storage applications.

They often are suitable for floor heating systems and operate at temperatures of approximately 45 and 25-35 °C [22, 23]. Previous researches have been demonstrated that the phase change temperatures of nanoconfined materials decrease [24-26]. In nanoconfined systems, the decrease in the phase change temperatures of organic PCMs are due to the confined subnanometerspaces that become narrower [27].

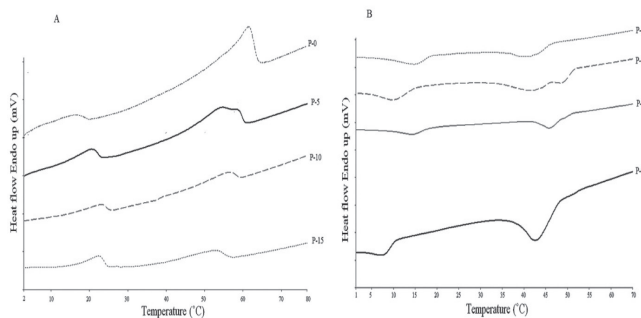


Figure 6. DSC curves of composite PCMs

The percentage of stearic acid (X) in PCMs (P-0, P-5, P-10 and P-15) was calculated by formula [28]

$$X\% = \frac{H}{H_0} * 100$$

Where H is the latent heat of PCM (J/g); H₀ is the latent heat of pure propargyl stearic acid (J/g). The percentages of stearic acid were 18, 16, 12 and 11.5 wt.% in P-0, P-5, P-10 and P-15, respectively. The theoretical melting enthalpy of the nanofibers can be calculated by formula [29]

$$HT = H_0 * \left(\frac{X}{1 - X} \right)$$

Where HT is for the theoretical melting enthalpy of PCM (J/g); H₀ is for the melting enthalpy of stearic propargyl ester; X is for the mass percentage of stearic propargyl ester in the PCM. By calculation, the theoretical melting enthalpy of nanofiber PCMs were about 58 J/g, 51 J/g, 36 J/g and 34 J/g for P-0, P-5, P-10 and P-15, respectively. Theoretical melting enthalpies were close to the measured melting enthalpies.

To confirm the prevention leakage, stearate acid and PCMs were heated to 100 °C. Figure 7 shows the digital photography of stearate ester and PCMs after heating at 100 °C for 2h. It can be seen that stearate ester completely melts and spreads onto the filter paper surface. However, UV-crosslinked PCMs no leakage was found. This means that P-0, P-5, P-10 and P-15 have well form stable performance.

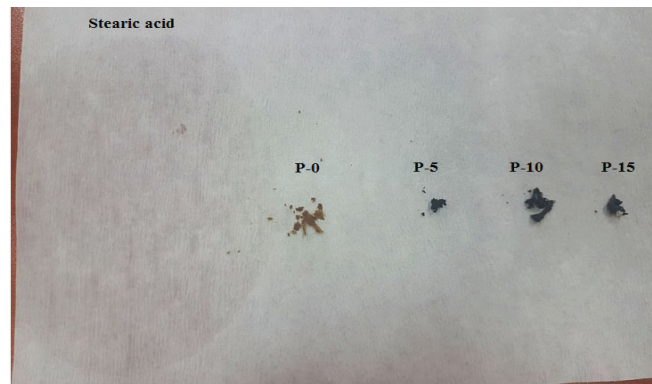


Figure 7. Photograph views of stearate ester and P-0, P-5, P-10 and P-15 after heating 100 °C

IV. CONCLUSIONS

In this study, stearic acid based composite phase change materials were prepared. Stearic ester was crosslinked with UV-induced thiol-yne click reaction to overcome the leakage problem of stearic acid. The leakage test indicated that UV-crosslinked stearate ester do not show leakage. TGA curves show that the addition of graphene oxide enhanced the thermal stability of composite PCMs. Furthermore, the composite PCMs have lowered the melting and freezing points compared to stearic acid. Therefore, it can be said that the composite PCMs can potentially be used as form-stable PCMs for lower temperature applications.

REFERENCES

- [1] Li, C., Xie, B., & Chen, J. (2017). Graphene-decorated silica stabilized stearic acid as a thermal energy storage material. *RSC Advances*, 7(48), 30142–30151.
- [2] Sharma, S. D., & Sagara, K. (2005). Latent Heat Storage Materials and Systems: A Review. *International Journal of Green Energy*, 2(1), 1–56.
- [3] Baetens, R., Jelle, B. P., & Gustavsen, A. (2010). Phase change materials for building applications: A state-of-the-art review. *Energy and Buildings*, 42(9), 1361–1368.
- [4] Baştürk, E., & Kahraman, M. V. (2016). Photocrosslinked-biobased phase change material for thermal energy storage. *Journal of Applied Polymer Science*, 133(32).
- [5] Grynning, S., Goia, F., Rognvik, E., & Time, B. (2013). Possibilities for characterization of a PCM window system using large scale measurements. *International Journal of Sustainable Built Environment*, 2(1), 56–64.
- [6] Alva, G., Huang, X., Liu, L., & Fang, G. (2017). Synthesis and characterization of microencapsulated myristic

- acid–palmitic acid eutectic mixture as phase change material for thermal energy storage. *Applied Energy*, 203, 677–685.
- [7] Zhang, T., Chen, M., Zhang, Y., & Wang, Y. (2017). Micro-encapsulation of stearic acid with polymethylmethacrylate using iron (III) chloride as photo-initiator for thermal energy storage. *Chinese Journal of Chemical Engineering*, 25(10), 1524–1532.
- [8] Döğüşcü, D. K., Altıntaş, A., Sarı, A., & Alkan, C. (2017). Polystyrene microcapsules with palmitic-capric acid eutectic mixture as building thermal energy storage materials. *Energy and Buildings*, 150, 376–382.
- [9] Feldman, D., Banu, D., & Hawes, D. (1995). Low chain esters of stearic acid as phase change materials for thermal energy storage in buildings. *Solar Energy Materials and Solar Cells*, 36(3), 311–322.
- [10] Cheng, X., Li, G., Yu, G., Li, Y., & Han, J. (2017). Effect of expanded graphite and carbon nanotubes on the thermal performance of stearic acid phase change materials. *Journal of Materials Science*, 52(20), 12370–12379.
- [11] Baştürk, E., & Kahraman, M. V. (2016). Photocrosslinked-biobased phase change material for thermal energy storage. *Journal of Applied Polymer Science*, 133(32), 43757–43765.
- [12] Baştürk, E., Deniz, D. Y., & Kahraman, M. V. (2016). Preparation of thiol-ene based photo-crosslinked polymer as a potential phase change material. *Materials Chemistry and Physics*, 177, 521–528.
- [13] Tiwari A, Syvajarvi M, editors. 2016 Advanced 2D materials. Hoboken, New Jersey: Scrivener Publishing, Wiley, 511 p.
- [14] Zhong, Y., Zhou, M., Huang, F., Lin, T., & Wan, D. (2013). Effect of graphene aerogel on thermal behavior of phase change materials for thermal management. *Solar Energy Materials and Solar Cells*, 113, 195–200.
- [15] Cui, Y., Liu, C., Hu, S., & Yu, X. (2011). The experimental exploration of carbon nanofiber and carbon nanotube additives on thermal behavior of phase change materials. *Solar Energy Materials and Solar Cells*, 95(4), 1208–1212.
- [16] Wang, J.-H., Cheng, C.-C., Yen, Y.-C., Miao, C.-C., & Chang, F.-C. (2012). Block-copolymer-like supramolecules confined in nanolamellae. *Soft Matter*, 8(14), 3747.
- [17] Anandhi, A., Palraj, S., Subramanian, G., & Selvaraj, M. (2016). Corrosion resistance and improved adhesion properties of propargyl alcohol impregnated mesoporous titanium dioxide built-in epoxy zinc rich primer. *Progress in Organic Coatings*, 97, 10–18.
- [18] Han, C., Liu, Y., Ma, J., & He, H. (2012). Key role of organic carbon in the sunlight-enhanced atmospheric aging of soot by O₂. *Proceedings of the National Academy of Sciences*, 109(52), 21250–21255.
- [19] Țucureanu, V., Matei, A., & Avram, A. M. (2016). FTIR Spectroscopy for Carbon Family Study. *Critical Reviews in Analytical Chemistry*, 46(6), 502–520.
- [20] Knothe, G., & Dunn, R. O. (2009). A Comprehensive Evaluation of the Melting Points of Fatty Acids and Esters Determined by Differential Scanning Calorimetry. *Journal of the American Oil Chemists' Society*, 86(9), 843–856.
- [21] Ye, S., Zhang, Q., Hu, D., & Feng, J. (2015). Core-shell-like structured graphene aerogel encapsulating paraffin: shape-stable phase change material for thermal energy storage. *Journal of Materials Chemistry A*, 3(7), 4018–4025.
- [22] Ding, L., Wang, L., Georgios, K., Lü, Y., & Zhou, W. (2017). Thermal characterization of lauric acid and stearic acid binary eutectic mixture in latent heat thermal storage systems with tube and fins. *Journal of Wuhan University of Technology-Mater. Sci. Ed.*, 32(4), 753–759.
- [23] Myhren, J. A., & Holmberg, S. (2008). Flow patterns and thermal comfort in a room with panel, floor and wall heating. *Energy and Buildings*, 40(4), 524–536.
- [24] Li, B., Liu, T., Hu, L., Wang, Y., & Nie, S. (2013). Facile preparation and adjustable thermal property of stearic acid–graphene oxide composite as shape-stabilized phase change material. *Chemical Engineering Journal*, 215–216, 819–826.
- [25] Karaman, S., Karaipekli, A., Sarı, A., & Biçer, A. (2011). Polyethylene glycol (PEG)/diatomite composite as a novel form-stable phase change material for thermal energy storage. *Solar Energy Materials and Solar Cells*, 95(7), 1647–1653.
- [26] Zhang, D., Tian, S., & Xiao, D. (2007). Experimental study on the phase change behavior of phase change material confined in pores. *Solar Energy*, 81(5), 653–660.
- [27] Uemura, T., Yanai, N., Watanabe, S., Tanaka, H., Numaguchi, R., Miyahara, M. T., Kitagawa, S. (2010). Unveiling thermal transitions of polymers in subnanometre pores. *Nature Communications*, 1(7), 1–8.
- [28] Fu, X., Liu, Z., Xiao, Y., Wang, J., & Lei, J. (2015). Preparation and properties of lauric acid/diatomite composites as novel form-stable phase change materials for thermal energy storage. *Energy and Buildings*, 104, 244–249.
- [29] He, H., Zhao, P., Yue, Q., Gao, B., Yue, D., & Li, Q. (2015). A novel polynary fatty acid/sludge ceramsite composite phase change materials and its applications in building energy conservation. *Renewable Energy*, 76, 45–52.